

IDENTIFYING OLIVINE COMPOSITION IN TYRRHENA TERRA, MARS, USING ORBITAL MID-INFRARED DATA. M. D. Lane¹, D. Tirsch², J. L. Bishop³, C. Viviano⁴, D. Loizeau⁵, L. L. Tornabene⁶, and R. Jaumann^{2,7} ¹Fibernetics LLC, Lititz, PA (lane@fibergyro.com), ²Institute of Planetary Research, German Aerospace Center (DLR), Berlin, Germany, ³Carl Sagan Center, SETI Institute, Mountain View, CA, USA, ⁴Dept. of Earth Sciences, Centre for Planetary Science and Exploration, University of Western Ontario, London, Canada, ⁵Johns Hopkins University Applied Physics Lab (JHUAPL), Laurel, Maryland, USA, ⁶University of Lyon, Lyon, France, ⁷Institute of Geological Sciences, Freie Universität Berlin, Berlin, Germany.

Introduction: Unaltered mafic rocks as well as a variety of aqueous alteration materials have been identified by investigations across the region between the Isidis and Hellas impact basins [e.g., 1-7]. Exposed views of ancient crustal rocks, lava flows from Syrtis Major, alteration from the Isidis and Hellas impact events and their overlapping ejecta, plus multiple stream beds and deltas make this region unique on Mars [e.g., 8-11] (Fig. 1). Previous studies of morphologic and spectroscopic features using coordinated NASA/ESA instrument data, including the Compact Reconnaissance Imaging Spectrometer for Mars (CRISM), High Resolution Stereo Camera (HRSC), High Resolution Imaging Science Experiment (HiRISE), and Context Camera (CTX) imagery, observed distinct stratigraphic units containing phyllosilicates, carbonate, olivine and pyroxene in isolated regions [e.g., 12-14].

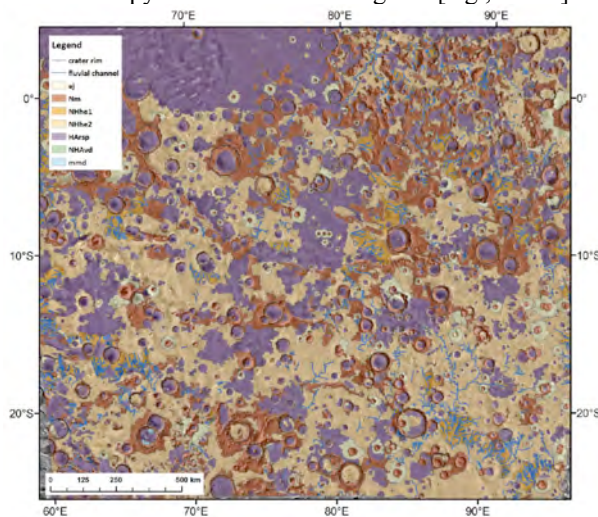


Figure 1. Geologic map of the study region spanning from southern Isidis Planitia to northern Hellas Planitia. From [13].

Bishop et al. [15] are studying a detailed region of Tyrrhena Terra to focus on alteration minerals and their geologic context using CRISM multispectral data (1.25 to 2.65 μm). In support of that work and to further understand the mineralogy and stratigraphic relationships of the broader Tyrrhena Terra region, this and future work will utilize the available longer-wavelength mid-infrared data from the Mars Global

Surveyor Thermal Emission Spectrometer (TES; 5.8 to 50 μm) and the Mars Odyssey Thermal Emission Imaging System (THEMIS; 6.8 to 14.9 μm) instruments. Our whole team also will be using spectral data sets from the visible (VIS) through the mid-infrared (MIR) and many other available Mars datasets to study the area.

TES Olivine Spectral Index: Olivine spectral indices were developed for spectra of 13 synthetic olivine pressed powders that ranged in composition from the Mg end member forsterite (Fo100) to the Fe end member fayalite (Fo0). Presentation of the entire range of Mg-Fe solid solution spectra can be found in [16]. By developing a spectral index that maps a feature that shifts with composition, Lane and Christensen [17] have previously applied the olivine indices to TES data using Java Mission-planning and Analysis for Remote Sensing (JMARS) software [18]. In [17], application of the olivine index to orbital data the Gale Crater dunes, allowed the olivine composition in the Bagnold Dunes to be identified as Fo55 (+/-5). This composition was verified on the ground by the *Curiosity* rover using CheMin data that identified the olivine as Fo56 (+/-3) [19].

Knowing that this methodology for determining olivine composition works well, the olivine indices were applied to TES data of our study site (and can be applied to any area on Mars). In order to apply the developed spectral indices to interpreting the TES data from Mars, the laboratory spectra (at 2 cm^{-1} spectral resolution) were degraded to the $\sim 10 \text{ cm}^{-1}$ spectral resolution to identify correct TES bands for the index formulae.

Fig. 2 shows the TES olivine index mapping of Fo50 in the top panel. Where more olivine of that composition is mapped, the pixels appear as warmer colors (toward red). Lesser (or no) olivine maps as cooler colors (toward blue).

TES Compositional Results: The TES data were used to create olivine composition index maps, and the best highlighted map (Fig. 2 top) suggests the Martian basaltic Tyrrhena Terra region is dominated by mid-range composition olivine (\sim Fo50). {A full range of other olivine compositions were mapped but are not shown here.} The bottom map shows the near-infrared-range CRISM data [20] where olivine is mapped in

green (Fe/Mg-bearing phyllosilicates are mapped in red; low-Ca pyroxene is mapped in blue). The locations of the mapped olivine correlate very well between the TES and CRISM data, and to Observatoire pour la Mineralogie, l'Eau, les Glaces et l'Activité (OMEGA) olivine data [7].

The TES olivine index maps are not designed to identify locations of phyllosilicates or pyroxenes; however, future work will be focused on mapping those minerals as well as the olivine using mid-infrared data in order to support the concurrent work of Bishop et al. [15].

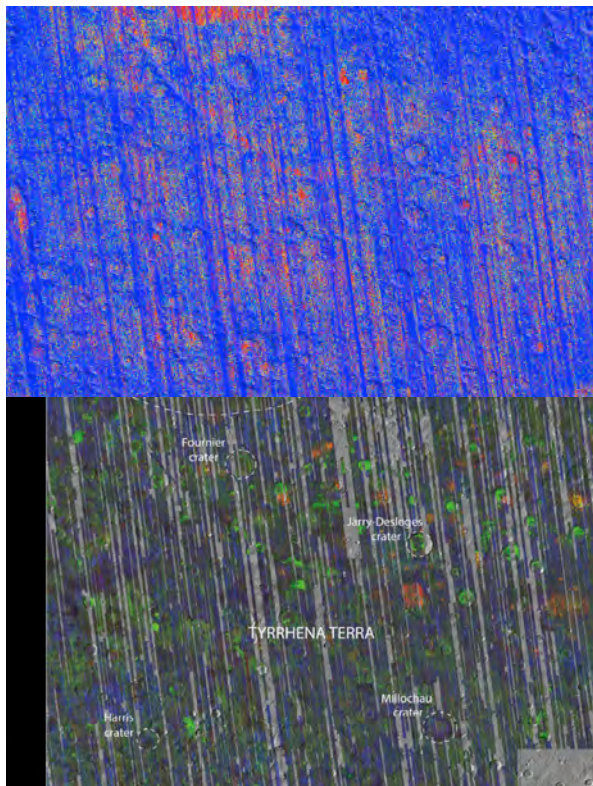


Figure 2. Top: Spectral index map of olivine (in red) for Fo50 as determined using TES data (~58 to 95 °E; 0 to 25 °S). Bottom: Red-Green-Blue (RGB) composite of CRISM data showing olivine mapped to green (phyllosilicates are orange/red; pyroxene is dark blue).

THEMIS Compositional Results: THEMIS decorrelation stretched (DCS) images are confirming our TES index maps of olivine locations. Using THEMIS bands 8, 7, and 5 assigned to red, green, and blue, olivine appears as magenta to purple. In Fig. 3, one area in Tyrrhena Terra identified using the TES olivine index also identifies the olivine in the higher spatial resolution THEMIS images.

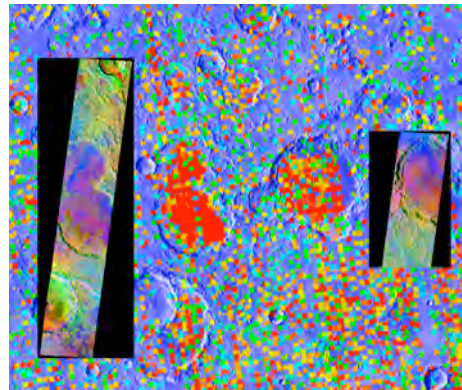


Figure 3. Olivine identified within craters (red) in the Oenotria Cavi area within Tyrrhena Terra. The background image is the TES Fo50 index. To the left and right (insets) are THEMIS DCS scenes (RGB=875) of these olivine-rich craters showing that olivine (purple) is also indicated.

Future Work: This and other regions will be studied in more detail using multiple data sets. Our team will be coordinating our multi-instrument and multi-wavelength spectral analyses to maximize the understanding of the primary and alteration geology of this region.

References: [1] Craddock R.A. (1994), *LPSC XXV*, Abstract #291. [2] Ivanov M.A. & Head J.W. (2003) *JGR*, 108, E6. [3] Rogers A.D. & Christensen P.R. (2007) *JGR*, 112, E01003. [4] Tornabene L.L. et al. (2008) *JGR*, 113, E10001. [5] Loizeau D. et al. (2012) *Icarus*, 219, 476-497. [6] Rogers A.D. & Hamilton V.E. (2015) *JGR*, 120, 62-91. [7] Ody et al. (2013) *JGR*, 118, 234-262. [8] Crumpler L.S. & Tanaka K.L. (2003) *JGR*, 108, 12. [9] Jaumann R., et al. (2010) *EPSL*, 294, 272-290. [10] Erkeling G., et al. (2012) *Icarus*, 219, 393-413. [11] Ivanov, M.A., et al. (2012) *Icarus*, 218, 24-46. [12] Bishop J.L., et al. (2013) *JGR*, 118, 487-513. [13] Tirsch, D., et al. (2018) *Icarus*, 314, 12-34. [14] Tirsch et al. (2019) 50th LPSC, Abstract #1532. [15] Bishop et al. (2020) 51st LPSC, Abstract #1811. [16] Lane et al. (2011) *JGR* 116, E08010. [17] Lane, M.D. & Christensen P.R. (2013) *GRL*, 40, 1-5. [18] Christensen P.R. et al. (2009) *EOS Trans. AGU*, 90(52), Fall Meet. Suppl., Abstract #IN22A-06. [19] Achilles C.N. et al. (2017) *JGR* 122, doi:10.1002/2017JE005262. [20] Murchie S.L., et al. (2009) *JGR*, 114, E00D06.

Acknowledgments: This work was funded through Mars Odyssey Participating Scientist sub-award 18-395 under grant 1228404 and Mars Data Analysis Program sub-award SC 3380 under grant 80NSSC18K1384.